Acta Crystallographica Section F
Structural Biology Communications
ISSN 2053-230X

Cloning, expression, purification, crystallization and preliminary X-ray diffraction analysis of *N*-acetylmannosamine-6-phosphate 2-epimerase from methicillin-resistant *Staphylococcus aureus*

Rachel A. North,[a] Sarah A. Kessans,[a] Michael D. W. Griffin,[b] Andrew J. A. Watson,[c] Antony J. Fairbanks[c] and Renwick C. J. Dobson[a,b]*

[a]Biomolecular Interaction Centre and School of Biological Sciences, University of Canterbury, Private Bag 4800, Christchurch 8041, New Zealand, [b]Department of Biochemistry and Molecular Biology, Bio21 Molecular Science and Biotechnology Institute, University of Melbourne, 30 Flemington Road, Parkville, Victoria 3010, Australia, and [c]Department of Chemistry, University of Canterbury, Private Bag 4800, Christchurch 8041, New Zealand

Correspondence e-mail: renwick.dobson@canterbury.ac.nz

Received 16 January 2014
Accepted 31 March 2014

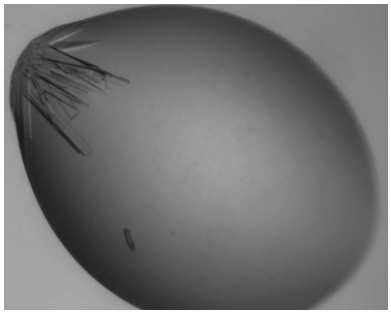

Sialic acids are one of the most important carbohydrate classes in biology. Some bacterial pathogens can scavenge sialic acids from their surrounding environment and degrade them as a source of carbon, nitrogen and energy. This sequestration and subsequent catabolism of sialic acid require a cluster of genes known as the 'Nan-Nag' cluster. The enzymes coded by these genes are important for pathogen colonization and persistence. Importantly, the Nan-Nag genes have proven to be essential for *Staphylococcus aureus* growth on sialic acids, suggesting that the pathway is a viable antibiotic drug target. The enzyme *N*-acetylmannosamine-6-phosphate 2-epimerase is involved in the catabolism of sialic acid; specifically, the enzyme converts *N*-acetylmannosamine-6-phosphate into *N*-acetylglucosamine-6-phosphate. The gene was cloned into an appropriate expression vector, and recombinant protein was expressed in *Escherichia coli* BL21 (DE3) cells and purified *via* a three-step procedure. Purified *N*-acetylmannosamine-6-phosphate 2-epimerase was screened for crystallization. The best crystal diffracted to a resolution of beyond 1.84 Å in space group $P2_12_12$. Understanding the structural nature of this enzyme from methicillin-resistant *S. aureus* will provide us with the insights necessary for the development of future antibiotics.

1. Introduction

Staphylococcus aureus is a Gram-positive bacterial pathogen that is the causative agent of a diverse range of clinical infections, particularly among those with compromised immune systems (Furuya & Lowy, 2006; Olson *et al.*, 2013). *S. aureus* is an extraordinarily adaptable pathogen that is notorious for its ability to evolve resistance mechanisms against novel antibiotics (Furuya & Lowy, 2006). As a result, the overall burden of antibiotic-resistant staphylococcal strains, particularly methicillin-resistant *S. aureus*, has reached epidemic proportions worldwide (Chambers & DeLeo, 2007; Grundmann *et al.*, 2006). The ever-increasing prevalence of this superbug and the continual progression of antibiotic resistance highlight the urgent need to characterize novel drug targets and develop new drugs against this pathogen. The enzymes involved in the catabolism of sialic acids are promising targets that have yet to be exploited.

Sialic acids (*e.g. N*-acetylneuraminic acid) constitute a large family of amino sugars that are found at the terminus of glycan molecules that are attached to the surface of eukaryotic cells (Vimr *et al.*, 2004). Interestingly, bacterial pathogens capable of colonizing heavily sialylated niches can scavenge sialic acid from their surrounding environment and degrade it as a source of carbon, nitrogen and energy (Almagro-Moreno & Boyd, 2009*a*; Vimr *et al.*, 2004). This sequestration and subsequent catabolism of sialic acid require a cluster of genes known as the 'Nan-Nag cluster' (Almagro-Moreno & Boyd, 2009*a*). The Nan-Nag cluster of genes encodes enzymes that scavenge sialic acid from the host, transport it into the bacterial cell and degrade it *via* a series of reactions into fructose-6-phosphate. This pathway has been documented in several bacterial pathogens and has proven to be necessary for colonization and persistence in mouse models for *Escherichia coli* (Chang *et al.*, 2004), *Vibrio cholerae* (Almagro-Moreno & Boyd, 2009*b*) and *V. vulnificus* (Jeong *et al.*, 2009). More significantly, the utilization of sialic acid as a carbon

source for growth has been proven for *S. aureus* (Olson *et al.*, 2013), making the pathway a viable target for drug design against this pathogen.

The sialic acid catabolic pathway is depicted in Fig. 1(*a*). The first committed step in the catabolism of sialic acid is the retro-aldol cleavage of *N*-acetylneuraminic acid by the enzyme *N*-acetylneuraminate lyase, removing a pyruvate group to yield *N*-acetyl-D-mannosamine (Barbosa *et al.*, 2000; Izard *et al.*, 1994; North *et al.*, 2013). *N*-Acetylmannosamine kinase then transfers a phosphate from adenosine-5′-triphosphate (ATP) to the C6 position of *N*-acetyl-D-mannosamine, generating *N*-acetylmannosamine-6-phosphate. Subsequently, *N*-acetylmannosamine-6-phosphate 2-epimerase converts *N*-acetylmannosamine-6-phosphate into *N*-acetylglucosamine-6-phosphate (detailed in Fig. 1*b*). Next, *N*-acetylglucosamine-6-phosphate deacetylase removes the acetyl group from *N*-acetylglucosamine-6-phosphate and yields glucosamine-6-phosphate. Glucosamine-6-phosphate deaminase then catalyses the isomerization and deamination of glucosamine-6-phosphate into fructose-6-phosphate (Almagro-Moreno & Boyd, 2009*a*).

Crystal structures of *N*-acetylmannosamine-6-phosphate 2-epimerase from methicillin-resistant *S. aureus* (PDB entry 1y0e; Midwest Center for Structural Genomics, unpublished work), *Salmonella enterica* (PDB entry 3igs; Center for Structural Genomics of Infectious Diseases, unpublished work) and *Streptococcus pyogenes* (PDB entry 1yxy; Midwest Center for Structural Genomics, unpublished work) have been solved and published in the PDB. However, these structures have not been published in the literature. Here, we present for the first time the cloning, expression, purification and preliminary X-ray diffraction analysis of *N*-acetylmannosamine-6-phosphate 2-epimerase from methicillin-resistant *S. aureus* USA300. The amino-acid sequence of PDB entry 1y0e differs from the construct presented in this article by only two residues. Firstly, PDB entry 1y0e contains an extra alanine residue at position 1, which precedes the methionine located at position 1 of the construct presented. Secondly, a valine residue located at position 220 of PDB entry 1y0e corresponds to an isoleucine residue located at position 219 of the construct presented.

2. Materials and methods

2.1. Sequence analysis of bacterial *N*-acetylmannosamine-6-phosphate 2-epimerase

A multiple protein sequence alignment was performed between *N*-acetylmannosamine-6-phosphate 2-epimerase from methicillin-resistant *S. aureus* USA300 (YP_493032), four additional Gram-positive bacterial species [*Clostridium botulinum* (WP_003363467), *Gemella haemolysans* (WP_003144293), *Lactobacillus plantarum* subsp. *plantarum* P-8 (YP_007988511) and *S. pneumoniae* (WP_000448318)] and six Gram-negative bacterial species [*E. coli* (WP_001261214), *Haemophilus influenzae* (WP_005691497), *S. enterica* subsp. *enterica* serovar Typhimurium strain LT2

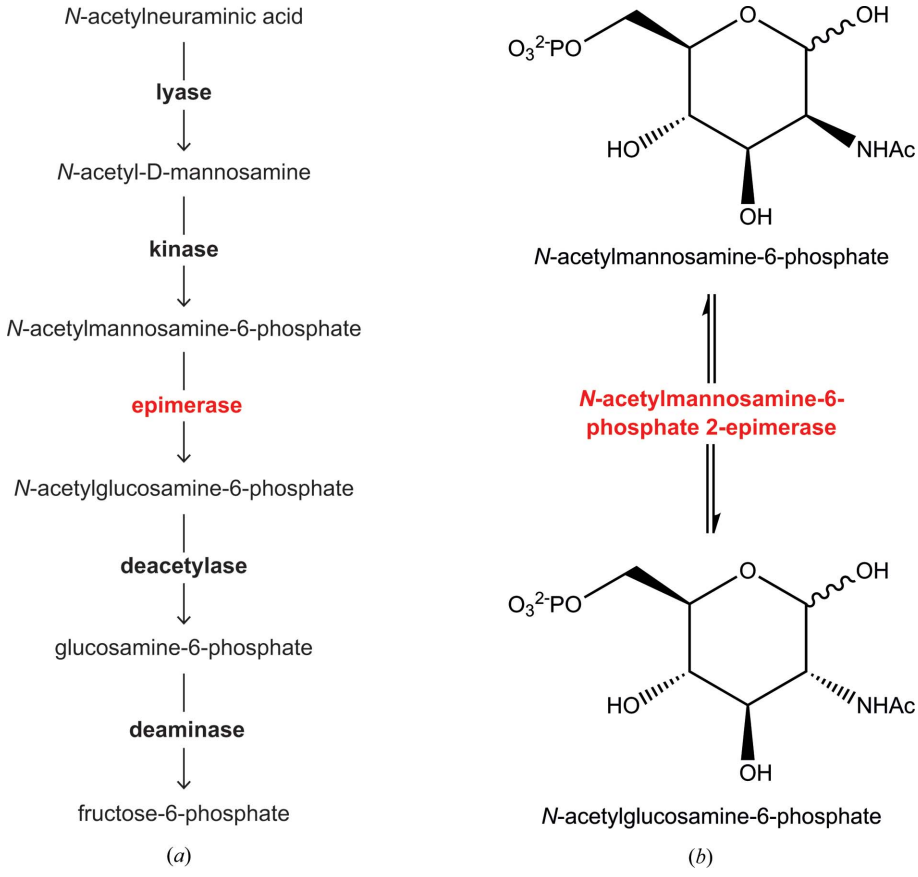

Figure 1
(*a*) Sialic acid catabolism. The enzymes involved in the uptake and subsequent catabolism of sialic acid are in bold. Lyase, *N*-acetylneuraminate lyase; kinase, *N*-acetylmannosamine kinase; epimerase (red), *N*-acetylmannosamine-6-phosphate 2-epimerase; deacetylase, *N*-acetylglucosamine-6-phosphate deacetylase; deaminase, glucosamine-6-phosphate deaminase. (*b*) The detailed reaction catalyzed by *N*-acetylmannosamine-6-phosphate 2-epimerase.

(NP_462247), *V. cholerae* (WP_002023168), *V. vulnificus* (WP_017421644) and *Yersinia pestis* KIM10+ (NP_668779)] (extracted from http://www.ncbi.nlm.hih.gov, protein accession numbers in parentheses). This alignment was performed using multiple sequence alignment by *ClustalW* (Larkin *et al.*, 2007; http://www.genome.jp/tools/clustalw/) with manual editing.

2.2. Cloning of *N*-acetylmannosamine-6-phosphate 2-epimerase

The *nanE* gene encoding *N*-acetylmannosamine-6-phosphate 2-epimerase from methicillin-resistant *S. aureus* USA300 (accession No. YP_493032) was synthesized commercially by GenScript and supplied in a cloning vector designated pUC57-Kan. *Nde*I and *Hin*dIII restriction sites were incorporated into the 5′ and 3′ ends of the *nanE* gene by the polymerase chain reaction (PCR) using the primer pair NanE-F (5′-CAT ATG TTA CCA CAT GGA TTA ATA GTA TCT TGT CAG GC-3′) and NanE-R (5′-AAG CTT TTA ATC TTC CAT AAT TTG AAC AAA ACG TTT CG-3′). The resulting PCR product was subcloned into pCR2.1-TOPO using a TOPO TA cloning kit (Invitrogen) to create pCR2.1-TOPO/NanE. The *nanE* gene was further subcloned into the pET30ΔSE expression vector (Suzuki *et al.*, 2014) by digestion with *Nde*I and *Hin*dIII restriction enzymes (New England Biolabs), purified using an agarose gel DNA extraction kit (Roche) and ligated with T4 DNA ligase at 293 K for 50 min to create pET30ΔSE/NanE.

2.3. Expression and purification

The recombinant expression vector was transformed into XL1-Blue competent cells and the plasmid DNA was successfully purified. Following sequence verification, plasmid DNA was transformed into *E. coli* BL21 (DE3) cells for protein overexpression. A single colony was transferred into 10 ml Luria broth containing 30 µg ml^{-1} kanamycin and cultured at 310 K and 180 rev min^{-1}. This culture was transferred into 2 l Luria broth containing 30 µg ml^{-1} kanamycin and grown for approximately 5 h at 310 K and 180 rev min^{-1} until an OD_{600} of 0.6 was reached. Expression of *N*-acetylmannosamine-6-phosphate 2-epimerase was induced by the addition of isopropyl β-D-1-thiogalactopyranoside to a final concentration of 1 m*M*, followed by further incubation overnight at 299 K and 180 rev min^{-1}. Cells were harvested by centrifugation using a Thermo Sorvall RC-6-Plus centrifuge for 10 min at 8000 rev min^{-1} and 277 K. The cells were then resuspended in buffer consisting of 20 m*M* Tris–HCl pH 8.0 and lysed by sonication using a Hielscher UP200S Ultrasonic Processor at 70% amplitude in cycles of 0.5 s on, 0.5 s off for 10 min. Cell debris was pelleted by centrifugation at 10 000 rev min^{-1} for 10 min at 277 K.

The cell lysate was first purified by anion-exchange chromatography. The soluble fraction was applied onto a 20 ml Q Sepharose column (GE Healthcare), which was pre-equilibrated with 20 m*M* Tris–HCl pH 8.0. The column was washed in this buffer until a steady baseline absorbance was observed. *N*-Acetylmannosamine-6-phosphate 2-epimerase was eluted *via* an increasing concentration gradient to 20 m*M* Tris–HCl pH 8.0, 1 *M* NaCl. Hydrophobic interaction chromatography was implemented as the second purification step; 1 *M* ammonium sulfate was added to the eluate of the anion-exchange step and applied onto a Phenyl Sepharose column (GE Healthcare), which was pre-equilibrated with 20 m*M* Tris–HCl pH 8.0, 1 *M* ammonium sulfate. The column was washed in this buffer until a steady baseline absorbance was observed. *N*-Acetylmannosamine-6-phosphate 2-epimerase was eluted using a decreasing concentration gradient of ammonium sulfate to 20 m*M* Tris–HCl pH 8.0. Size-exclusion chromatography was employed as the final purification step using a HiLoad 16/60 Superdex 200 column (GE Healthcare) with 20 m*M* Tris–HCl pH 8.0. All purification steps were carried out at 277 K. *N*-Acetylmannosamine-6-phosphate 2-epimerase was concentrated using a 10 kDa molecular-weight cutoff Centricon (Millipore). Protein concentration was determined after each purification step using the Bradford assay (Bradford, 1976).

2.4. Crystallization of *N*-acetylmannosamine-6-phosphate 2-epimerase

Crystallization studies were initially conducted using a 10 mg ml^{-1} preparation of *N*-acetylmannosamine-6-phosphate 2-epimerase from

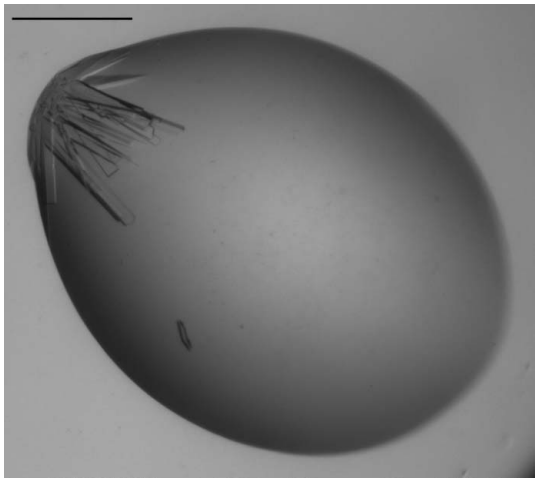

Figure 2
Crystallization of *N*-acetylmannosamine-6-phosphate 2-epimerase from methicillin-resistant *S. aureus*. Crystals from condition E1 of The JCSG+ Suite. The scale bar indicates 0.3 mm.

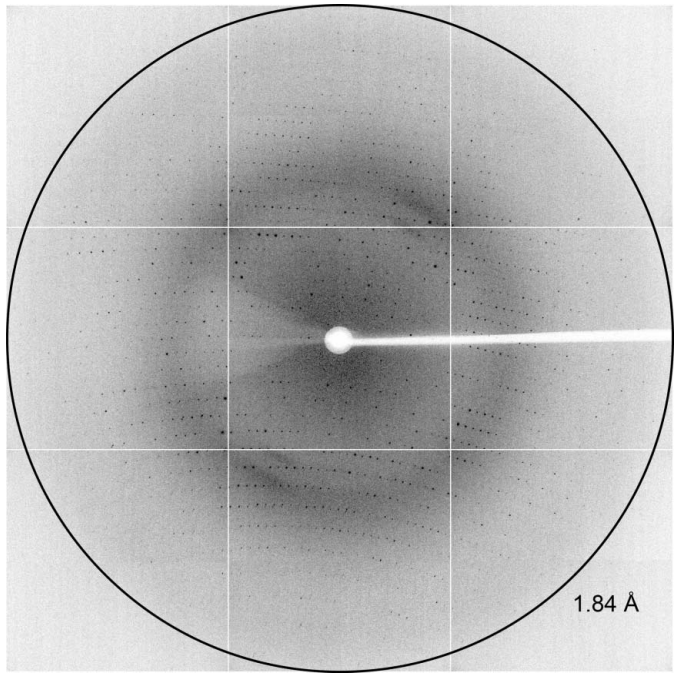

Figure 3
X-ray diffraction of *N*-acetylmannosamine-6-phosphate 2-epimerase from methicillin-resistant *S. aureus*. Diffraction to 1.84 Å resolution is marked with a ring.

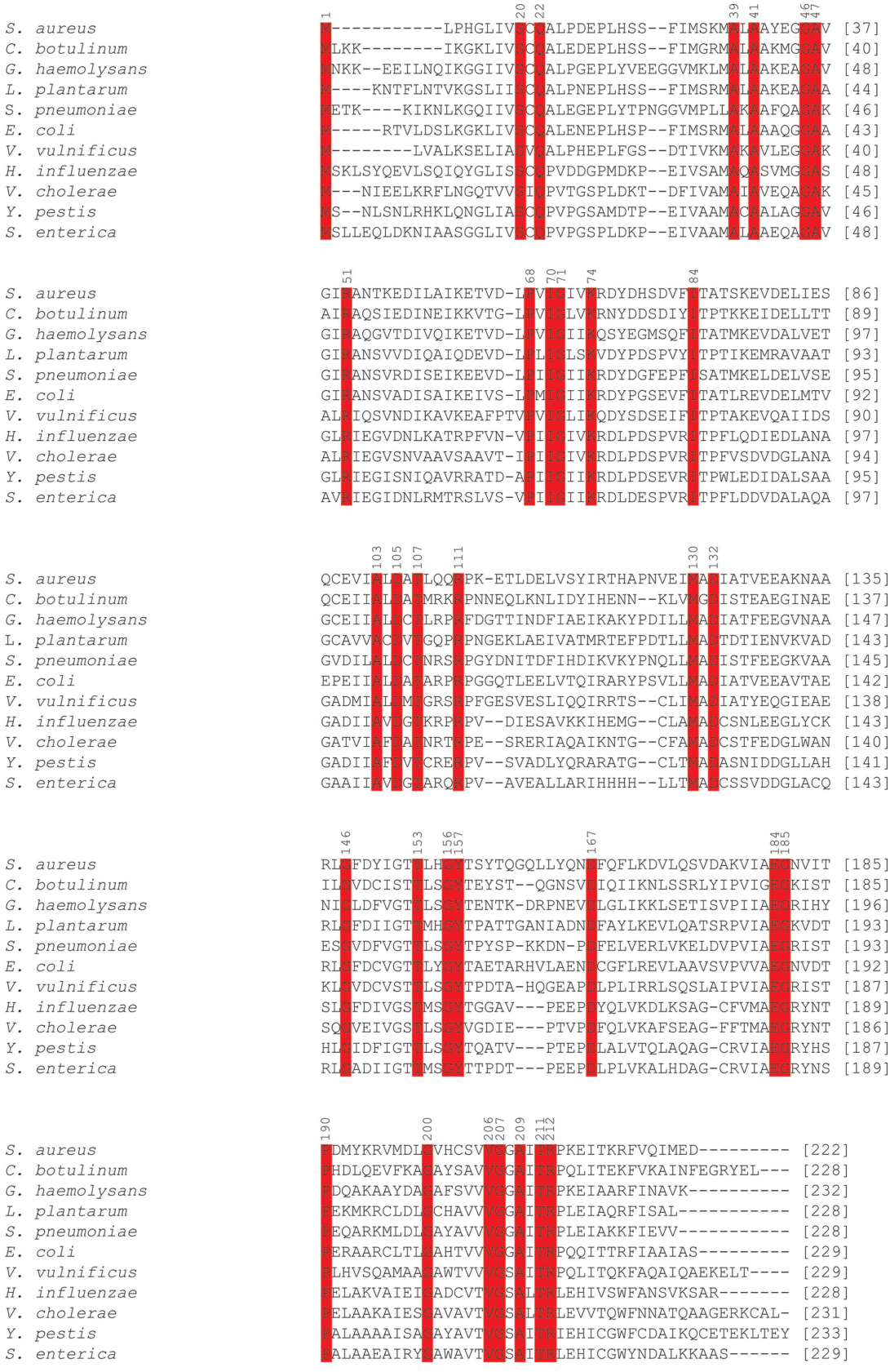

Figure 4
Sequence alignment of *N*-acetylmannosamine-6-phosphate 2-epimerase from five Gram-positive and six Gram-negative species of bacteria. Highly conserved residues are highlighted in red. Conserved amino-acid residues are numbered according to *S. enterica*.

methicillin-resistant *S. aureus* in 20 m*M* Tris–HCl pH 8.0. Initial protein crystallization trials were performed at the Collaborative Crystallization Centre (C3; http://www.csiro.au/c3/) using The PACT Suite and The JCSG+ Suite crystal screens (Newman *et al.*, 2005, 2008) at 281 and 293 K. Crystal screens were performed using the sitting-drop vapour-diffusion method with droplets consisting of 150 nl protein solution and 150 nl reservoir solution. The JCSG+ Suite produced crystals in several of the screen conditions. Condition E1 (1 *M* trisodium citrate, 0.1 *M* sodium cacodylate pH 6.5) produced crystals in a cluster after 1 d at 281 K (Fig. 2). These crystals were suitable for the collection of high-resolution X-ray diffraction data.

2.5. Data collection and processing

High-quality X-ray diffraction data (Fig. 3) were collected on the MX2 beamline at the Australian Synchrotron, Victoria, Australia. Crystals from The JCSG+ Suite condition E1 were briefly soaked in cryoprotectant solution containing 85% reservoir solution (1 *M* trisodium citrate, 0.1 *M* sodium cacodylate pH 6.5) and 15% of a 1:1 ethylene glycol:glycerol mixture, mounted onto a Cryo-Loop (Hampton Research) and flash-cooled in liquid nitrogen. Crystals were mounted onto the beamline in a stream of nitrogen gas at 110 K. The ADSC Quantum 315r detector was positioned 280 mm from the crystal and data were collected in 0.5° increments for one 180° pass, with 90% attenuation and an exposure time of 1 s.

The data were indexed and integrated using *xdsme* (Kabsch, 2010). Scaling and data reduction were then performed using *AIMLESS* (Evans, 2006, 2011) from the *CCP*4 program suite (Winn *et al.*, 2011). The resulting intensity data were analyzed using *phenix.xtriage* (Adams *et al.*, 2010). Molecular replacement was performed using the program *Phaser* (McCoy *et al.*, 2007) *via CCP*4. The monomer of *S. aureus N*-acetylmannosamine-6-phosphate 2-epimerase (PDB entry 1y0e) was used as the search model. The resulting structure is currently being rebuilt using *Coot* (Emsley *et al.*, 2010) and refined using both *REFMAC* (Murshudov *et al.*, 1997, 2011) and *phenix.refine* (Afonine *et al.*, 2012). All relevant data-collection and processing parameters are given in Table 1. Images will be made available *via* the TARDIS server (Androulakis *et al.*, 2008) when the structure is published.

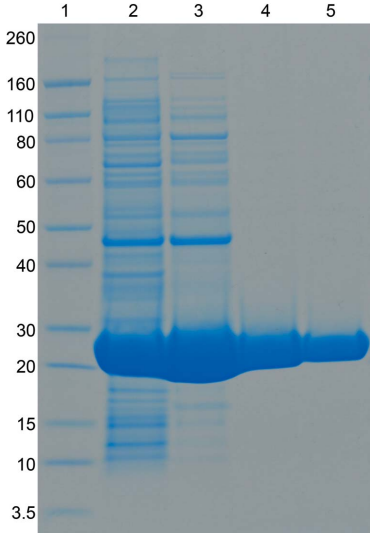

Figure 5
Purification of recombinant *N*-acetylmannosamine-6-phosphate 2-epimerase from methicillin-resistant *S. aureus*. Lane 1, molecular-weight markers (labelled in kDa); lane 2, crude cell lysate; lane 3, pooled fractions from the anion-exchange chromatography step; lane 4, pooled fractions from the hydrophobic interaction chromatography step; lane 5, pooled fractions from the size-exclusion chromatography step.

Table 1
X-ray data-collection statistics for *N*-acetylmannosamine-6-phosphate 2-epimerase from methicillin-resistant *S. aureus*.

Values in parentheses are for the highest resolution shell. The Matthews coefficient and solvent content are based on two monomers, with a combined molecular weight of 49 090 Da, in the asymmetric unit.

Wavelength (Å)	0.9537
No. of images	360
Oscillation range (°)	0.5
Space group	$P2_12_12$
Unit-cell parameters (Å, °)	a = 77.1, b = 173.7, c = 44.4, $\alpha = \beta = \gamma$ = 90
Resolution (Å)	46.3–1.84 (1.88–1.84)
Observed reflections	189024 (9200)
Unique reflections	52704 (3125)
Completeness (%)	99.8 (98.5)
$R_{\rm merge}$†	0.082 (0.549)
$R_{\rm r.i.m.}$‡	0.112 (0.738)
$R_{\rm p.i.m.}$§	0.076 (0.490)
Mean $I/\sigma(I)$	10.8 (1.8)
Multiplicity	3.6 (2.9)
Wilson B value (Å^2)	9.6
Molecules in asymmetric unit	2
$V_{\rm M}$ (Å^3 Da^{-1})	3.04
Solvent content (%)	59.5

† $R_{\rm merge} = \sum_{hkl}\sum_i |I_i(hkl) - \langle I(hkl)\rangle| / \sum_{hkl}\sum_i I_i(hkl)$. ‡ $R_{\rm r.i.m.} = \sum_{hkl}\{N(hkl)/[N(hkl)-1]\}^{1/2}\sum_i |I_i(hkl) - \langle I(hkl)\rangle| / \sum_{hkl}\sum_i I_i(hkl)$. § $R_{\rm p.i.m.} = \sum_{hkl}\{1/[N(hkl)-1]\}^{1/2}\sum_i |I_i(hkl) - \langle I(hkl)\rangle| / \sum_{hkl}\sum_i I_i(hkl)$, where $I_i(hkl)$ is the ith intensity measurement of reflection hkl, $\langle I(hkl)\rangle$ is its average and $N(hkl)$ is the redundancy of a given reflection.

3. Results and discussion

3.1. Sequence analysis of bacterial *N*-acetylmannosamine-6-phosphate 2-epimerase

A multiple protein sequence alignment was performed between *N*-acetylmannosamine-6-phosphate 2-epimerase from methicillin-resistant *S. aureus*, four additional Gram-positive bacterial species (*C. botulinum*, *G. haemolysans*, *L. plantarum* and *S. pneumoniae*) and six Gram-negative bacterial species (*E. coli*, *H. influenzae*, *S. enterica*, *V. cholerae*, *V. vulnificus* and *Y. pestis*). This was performed to investigate the homology of *N*-acetylmannosamine-6-phosphate 2-epimerase from methicillin-resistant *S. aureus* with additional Gram-positive and Gram-negative bacterial species. Furthermore, such sequence analysis may allow the identification of amino-acid residues that are potentially involved in catalysis. Owing to a lack of literature published on *N*-acetylmannosamine-6-phosphate 2-epimerase, it is difficult to predict which residues are involved in catalysis. However, the crystal structure of *N*-acetylmannosamine-6-phosphate 2-epimerase from *S. enterica* with a bound ligand, *N*-acetylglucosmine-6-phosphate, has been solved (PDB entry 3igs). Here, *N*-acetylglucosamine-6-phosphate is predicted to form hydrogen bonds to Arg83 and Lys74 (amino-acid numbering corresponds to that of *S. enterica*). As illustrated in Fig. 4, Lys74 is conserved between all of the Gram-positive and Gram-negative bacterial species analyzed. In contrast, Arg83 is only highly conserved between *S. enterica*, *H. influenzae*, *V. cholerae* and *Y. pestis*. *S. aureus* and the remaining organisms have either a phenylalanine or a tyrosine residue in this position. The strict conservation of Lys74 indicates that this residue is likely to be important for the function of *N*-acetylmannosamine-6-phosphate 2-epimerase. Ligand-bound crystal structures of

N-acetylmannosamine-6-phosphate 2-epimerase from methicillin-resistant *S. aureus* will further confirm this.

3.2. Expression and purification of *N*-acetylmannosamine-6-phosphate 2-epimerase

Purification of methicillin-resistant *S. aureus* *N*-acetylmannosamine-6-phosphate 2-epimerase was carried out using anion-exchange chromatography, hydrophobic interaction chromatography and size-exclusion chromatography. From 2 l of bacterial cell culture, approximately 370 mg protein was obtained after anion-exchange chromatography, 200 mg after hydrophobic interaction chromatography and 140 mg after size-exclusion chromatography. The purity of the sample following size-exclusion chromatography was at least 95%, as estimated by SDS–PAGE (Fig. 5).

3.3. Crystallization, data collection and processing of *N*-acetylmannosamine-6-phosphate 2-epimerase

X-ray diffraction data were collected to a resolution of 1.84 Å from a crystal that grew in condition E1 of The JCSG+ Suite in a screen perfomed at C3. The crystal grew as a cluster, which was broken apart prior to mounting it into the nylon loop. The crystal was very delicate and crushed easily, so great care was required. Analysis of the intensity data using *POINTLESS* (Evans, 2006) suggested that the crystals belong to the orthorhombic space group $P2_12_12$. The presence of two screw axes was verified by the presence of systematic absences in only two of the axes. The Matthews coefficient (Matthews, 1968) was estimated to be 3.04 $Å^3\ Da^{-1}$ with a corresponding solvent content of 59.5%; this assumes two monomers in the asymmetric unit that form a dimer. Molecular replacement was conducted using the program *Phaser* with data scaled in $P2_12_12$. The monomer of *S. aureus* *N*-acetylmannosamine-6-phosphate 2-epimerase (PDB entry 1y0e) was used as the search model, producing a final solution with a translation-function *Z*-score of 38.1 and a log-likelihood gain of 8222. The construct presented in this article differs by only two amino-acid residues from that of PDB entry 1y0e, yet our structure has a unique cell and symmetry; PDB entry 1y0e has space group $P2_12_12_1$ and the unit-cell parameters are $a = 53.0$, $b = 76.3$, $c = 183.66$ Å, $\alpha = \beta = \gamma = 90.0^\circ$. Structure determination is currently under way.

In summary, the cloning, expression, purification, crystallization and preliminary X-ray diffraction analysis of *N*-acetylmannosamine-6-phosphate 2-epimerase from methicillin-resistant *S. aureus* USA300 are presented for the first time.

We acknowledge the support and assistance of the friendly staff at the CSIRO Collaborative Crystallization Centre at CSIRO Material Science and Engineering, Parkville, Melbourne and the MX beamline scientists at the Australian Synchrotron, Victoria, Australia. Parts of this research were undertaken at the MX2 beamline of the Australian Synchrotron. Travel to the Australian Synchrotron was supported by the New Zealand Synchrotron Group. RCJD acknowledges the following for funding support, in part: (i) the Ministry of Business, Innovation and Employment (contract UOCX1208); (ii) the New Zealand Royal Society Marsden Fund (contract UOC1013); and (iii) the US Army Research Laboratory and US Army Research Office under contract/grant No. W911NF-11-1-0481. We especially thank Jackie Healy for her steely technical support.

References

Adams, P. D. *et al.* (2010). *Acta Cryst.* D**66**, 213–221.
Afonine, P. V., Grosse-Kunstleve, R. W., Echols, N., Headd, J. J., Moriarty, N. W., Mustyakimov, M., Terwilliger, T. C., Urzhumtsev, A., Zwart, P. H. & Adams, P. D. (2012). *Acta Cryst.* D**68**, 352–367.
Almagro-Moreno, S. & Boyd, E. F. (2009*a*). *BMC Evol. Biol.* **9**, 118.
Almagro-Moreno, S. & Boyd, E. F. (2009*b*). *Infect. Immun.* **77**, 3807–3816.
Androulakis, S. *et al.* (2008). *Acta Cryst.* D**64**, 810–814.
Barbosa, J. A., Smith, B. J., DeGori, R., Ooi, H. C., Marcuccio, S. M., Campi, E. M., Jackson, W. R., Brossmer, R., Sommer, M. & Lawrence, M. C. (2000). *J. Mol. Biol.* **303**, 405–421.
Bradford, M. M. (1976). *Anal. Biochem.* **72**, 248–254.
Chambers, H. F. & DeLeo, F. R. (2007). *Nature Rev. Microbiol.* **7**, 629–641.
Chang, D. E., Smalley, D. J., Tucker, D. L., Leatham, M. P., Norris, W. E., Stevenson, S. J., Anderson, A. B., Grissom, J. E., Laux, D. C., Cohen, P. S. & Conway, T. (2004). *Proc. Natl Acad. Sci. USA*, **101**, 7427–7432.
Emsley, P., Lohkamp, B., Scott, W. G. & Cowtan, K. (2010). *Acta Cryst.* D**66**, 486–501.
Evans, P. (2006). *Acta Cryst.* D**62**, 72–82.
Evans, P. R. (2011). *Acta Cryst.* D**67**, 282–292.
Furuya, E. Y. & Lowy, F. D. (2006). *Nature Rev. Microbiol.* **4**, 36–45.
Grundmann, H., Aires-de-Sousa, M., Boyce, J. & Tiemersma, E. (2006). *Lancet*, **368**, 874–885.
Izard, T., Lawrence, M. C., Malby, R. L., Lilley, G. G. & Colman, P. M. (1994). *Structure*, **2**, 361–369.
Jeong, H. G., Oh, M. H., Kim, B. S., Lee, M. Y., Han, H. J. & Choi, S. H. (2009). *Infect. Immun.* **77**, 3209–3217.
Kabsch, W. (2010). *Acta Cryst.* D**66**, 125–132.
Larkin, M. A., Blackshields, G., Brown, N. P., Chenna, R., McGettigan, P. A., McWilliam, H., Valentin, F., Wallace, I. M., Wilm, A., Lopez, R., Thompson, J. D., Gibson, T. J. & Higgins, D. G. (2007). *Bioinformatics*, **23**, 2947–2948.
Matthews, B. W. (1968). *J. Mol. Biol.* **33**, 491–497.
McCoy, A. J., Grosse-Kunstleve, R. W., Adams, P. D., Winn, M. D., Storoni, L. C. & Read, R. J. (2007). *J. Appl. Cryst.* **40**, 658–674.
Murshudov, G. N., Skubák, P., Lebedev, A. A., Pannu, N. S., Steiner, R. A., Nicholls, R. A., Winn, M. D., Long, F. & Vagin, A. A. (2011). *Acta Cryst.* D**67**, 355–367.
Murshudov, G. N., Vagin, A. A. & Dodson, E. J. (1997). *Acta Cryst.* D**53**, 240–255.
Newman, J., Egan, D., Walter, T. S., Meged, R., Berry, I., Ben Jelloul, M., Sussman, J. L., Stuart, D. I. & Perrakis, A. (2005). *Acta Cryst.* D**61**, 1426–1431.
Newman, J., Pham, T. M. & Peat, T. S. (2008). *Acta Cryst.* F**64**, 991–996.
North, R. A., Kessans, S. A., Atkinson, S. C., Suzuki, H., Watson, A. J. A., Burgess, B. R., Angley, L. M., Hudson, A. O., Varsani, A., Griffin, M. D. W., Fairbanks, A. J. & Dobson, R. C. J. (2013). *Acta Cryst.* F**69**, 306–312.
Olson, M. E., King, J. M., Yahr, T. L. & Horswill, A. R. (2013). *J. Bacteriol.* **195**, 1779–1788.
Suzuki, H., Tabata, K., Morita, E., Kawasaki, M., Kato, R., Dobson, R. C. J., Yoshimori, T. & Wakatsuki, S. (2014). *Structure*, **22**, 47–58.
Vimr, E. R., Kalivoda, K. A., Deszo, E. L. & Steenbergen, S. M. (2004). *Microbiol. Mol. Biol. Rev.* **68**, 132–153.
Winn, M. D. *et al.* (2011). *Acta Cryst.* D**67**, 235–242.